

CASE REPORT

Open Access



Phosphaturic mesenchymal tumor of the skull base presenting with tumor-induced osteomalacia and multiple fractures: a case report

He Zhiqing¹, Wang Keshuang², Zhang Minghui³, Qin Jiace³ and Qiu Qianhui^{1,2*} 

Abstract

Background This case reports a rare disease in which the clinical symptoms are completely inconsistent with the primary site. As the occurrence of this disease is partly rare, the challenges in the diagnosis of phosphaturic mesenchymal tumors are discussed. It also provides a new clinical treatment option, that is, the combined treatment with anlotinib capsules after surgery and the long-term follow-up to observe the effect of the combined treatment.

Case presentation A 27-year-old Chinese woman presented with generalized pain and multiple fractures for 2 years. The present case was initially thought to be hematogenous and involved a malignant predisposition. After initial positron emission tomography-computed tomography imaging, endoscopic resection of the lesion was performed, and a biopsy confirmed the diagnosis of phosphaturic mesenchymal tumor. Following pathological confirmation, the patient was treated with anlotinib capsules. Post-treatment, the patient regained the ability to walk. The patient was monitored for 2 years, during which time no recurrence was observed.

Conclusions Phosphaturic mesenchymal tumors include rare cranial base neoplasms that are often overlooked due to their nonspecific symptoms. Accurate diagnosis requires a comprehensive assessment, encompassing systemic evaluation, laboratory tests, imaging studies, and microscopic examination. This case demonstrates the innovative use of anlotinib capsules in the treatment of PMTs. After 2 years, no recurrence was observed, and the patient returned to normal life. Effective management of this condition necessitates a multidisciplinary approach involving otolaryngologists, radiologists, nuclear medicine specialists, and pathologists.

Keywords Phosphaturic mesenchymal tumors, Case report, Otolaryngology department

*Correspondence:

Qiu Qianhui

qiuqianhui@gdph.org.cn

¹ Department of Otolaryngology-Head and Neck Surgery, Guangdong Cardiovascular Institute, Guangdong Provincial People's Hospital, Guangdong Academy of Medical Sciences, Guangzhou, China

² Department of Otolaryngology-Head and Neck Surgery, Guangdong Provincial People's Hospital (Guangdong Academy of Medical Sciences), Southern Medical University, Guangzhou, China

³ Pathology Department, Guangdong Provincial People's Hospital (Guangdong Academy of Medical Sciences), Southern Medical University, Guangzhou, China

Background

Phosphaturic mesenchymal tumors (PMTs) reported in skull base are a kind of rare disease, typically representing cases of tumor-induced osteomalacia (TIO) associated with mesenchymal tumors originating from a single entity. TIO is associated with cancer in only a few cases; however, it has become increasingly clear in recent years that osteomalacia caused by mesenchymal tumors almost always pertains to a tumor with unique morphological and genetic characteristics [1]. Osteomalacia refers to insufficient or delayed mineralization



of osteoid tissue in mature bone. Therefore, the main clinical symptoms include muscle pain and progressive weakness, often lasting for months or years. PMTs can also cause TIO, and a recent study reported that the average time from symptom onset to diagnosis of osteomalacia was 3 years, consistent with this case [2]. Furthermore, phosphaturic mesenchymal tumors almost invariably present with chronic hypophosphatemia rather than symptoms directly related to the tumor itself. Similar to osteomalacia caused by other factors, skeletal pain and fractures may occur as the disease progresses. The disease site is typically identified through PET-CT when multiple fractures occur throughout the body.

PMTs predominantly occur in middle-aged individuals, although extremely rare cases have been reported in infants and the elderly [3]. PMTs can occur almost anywhere in soft tissues or bones but are most common in the extremities [4], especially their distal parts, and less so in the head and neck, where they tend to be benign and associated with TIO syndrome, particularly in the paranasal sinuses [5]. According to 2022 data, only 5% of PMT cases occur in craniofacial regions, making initial diagnosis challenging. The vast majority of phosphaturic mesenchymal tumors are benign, and hypophosphatemia and osteomalacia can gradually improve after complete resection. However, the reported recurrence rate of PMTs ranges from 0% to 57%, with local recurrence often linked to incomplete resection, surgical experience, and the extent of resection margins [6]. Additionally, there has been a report of a histologically benign tumor metastasizing to the lungs [7].

Case presentation

A female patient aged 27 years resented with a 2-year history of bone pain in the lumbosacral region and both lower legs; 3 months before admission, the patient developed a pathological fracture of the pelvis, as the pain in her lower limbs and back progressively worsened, limiting her ability to walk and turn over in bed. Pharmacological treatments aimed at protecting bone health were ineffective (Fig. 1), and she eventually became wheelchair-bound.

One month before admission, positron emission tomography-computed tomography (PET-CT) revealed soft tissue thickening (14 mm × 7 mm) with high somatostatin receptor expression in the right skull base, suggestive of a neuroendocrine tumor, and widespread bone lesions with abnormal metabolism and destruction, indicative of metabolic bone disease.

The patient presented to Department of Otorhinolaryngology for treatment due to a skull base mass discovered by PET-CT. There was no history of nasal obstruction, rhinorrhea, epistaxis, or hyposmia. Otorhinolaryngological examination did not reveal any positive signs, and there was no history of trauma or relevant hereditary diseases in the family. Laboratory tests showed a serum calcium level of 2.73 mmol/L (normal range: 2.11–2.52 mmol/L), phosphate level <0.32 mmol/L (normal range: 0.85–1.51 mmol/L), and alkaline phosphatase (ALP) level of 381 U/L (normal range: 35–100 U/L); other blood tests were within normal limits. Magnetic resonance imaging (MRI) of the nasopharynx and cranial base with and without contrast revealed a round lesion approximately 14 mm × 7 mm in size located in the right pterygopalatine fossa, showing isointense signal on T1-weighted images, slightly hyperintense signal on T2-weighted images, and markedly homogeneous enhancement on

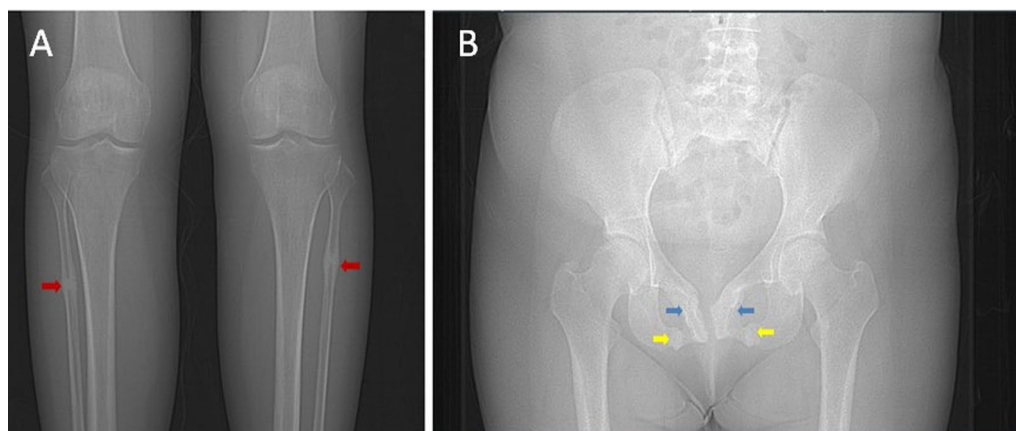


Fig. 1 Multiple fracture radiographic imaging demonstrating irregular bone morphology with callus formation in the bilateral inferior pubic rami (**B** blue arrows), ischium (**B** yellow arrows), and proximal fibulae (**A** red arrows)

post-contrast imaging, suggesting a high possibility of a neuroendocrine tumor (Fig. 2).

Endoscopic transnasal resection of the skull base lesion: intraoperatively, the lesion was found adherent to the dura mater of the skull base, exhibiting expansive growth. The tumor was approximately 1.5 cm in diameter, gray-white in color, soft in consistency, and well vascularized. It was completely excised under direct visualization.

On postoperative day 5, the serum phosphate level was 0.53 mmol/L (normal range: 0.85–1.51 mmol/L), and the serum calcium level had returned to the normal range. At discharge, the patient reported some relief from bone pain.

Immunohistochemistry demonstrated positivity staining for vimentin (+ +), SSTR2 (+ + +), ERG (+ +), CD56 (+ +), and SATB2 (+ + +), while negative for CD34, STAT6, S100, and CgA. On the basis of the

immunoreactivity of CD56, the possibility of EWSR1 and SYT gene breakage was proposed. Gene testing and immunohistochemistry for CD99 on the tissue sample were both negative, ruling out the diagnosis of Ewing's sarcoma and synovial sarcoma. Considering the cytology of the cells as mild spindle cells, rich interstitial vessels, and strong immunoreactivity of ERG, PMT was considered, SATB2 and SSTR2 was performed, which showed strong expression for the two markers. Combined with the manifestation of systemic hypophosphatemia, the pathological diagnosis of PMT was confirmed (Fig. 3).

At 2 months after surgery, pending pathological confirmation, the patient was treated with sodium clodronate injection (10 mg) to alleviate bone pain. Targeted drug regimens were provided to patients and their families, and both parties agreed to proceed. For targeted therapy, anlotinib capsules at a dose of 12 mg were prescribed

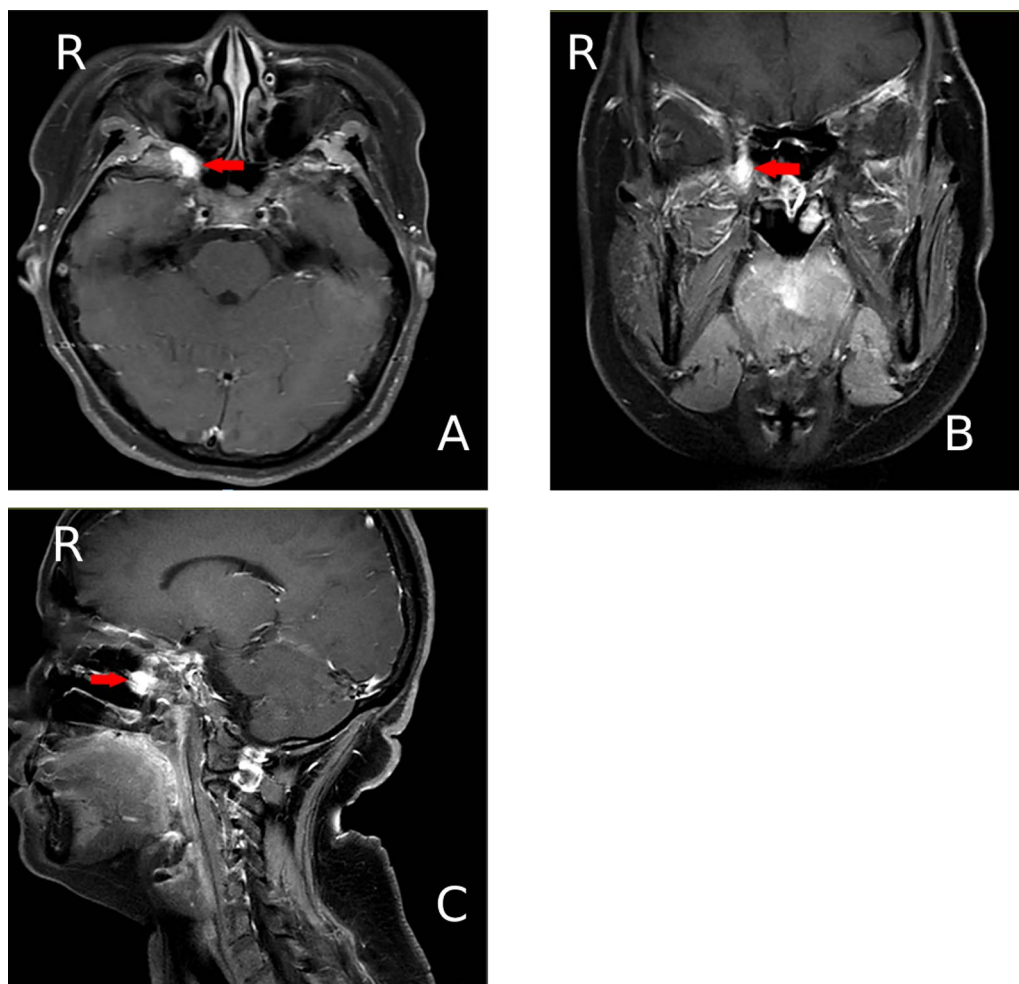


Fig. 2 Magnetic resonance imaging with and without contrast enhancement showing a round area of abnormal signal (as indicated by arrow) in the right pterygopalatine fossa, measuring approximately 14 mm × 7 mm (The arrows point to the tumor)

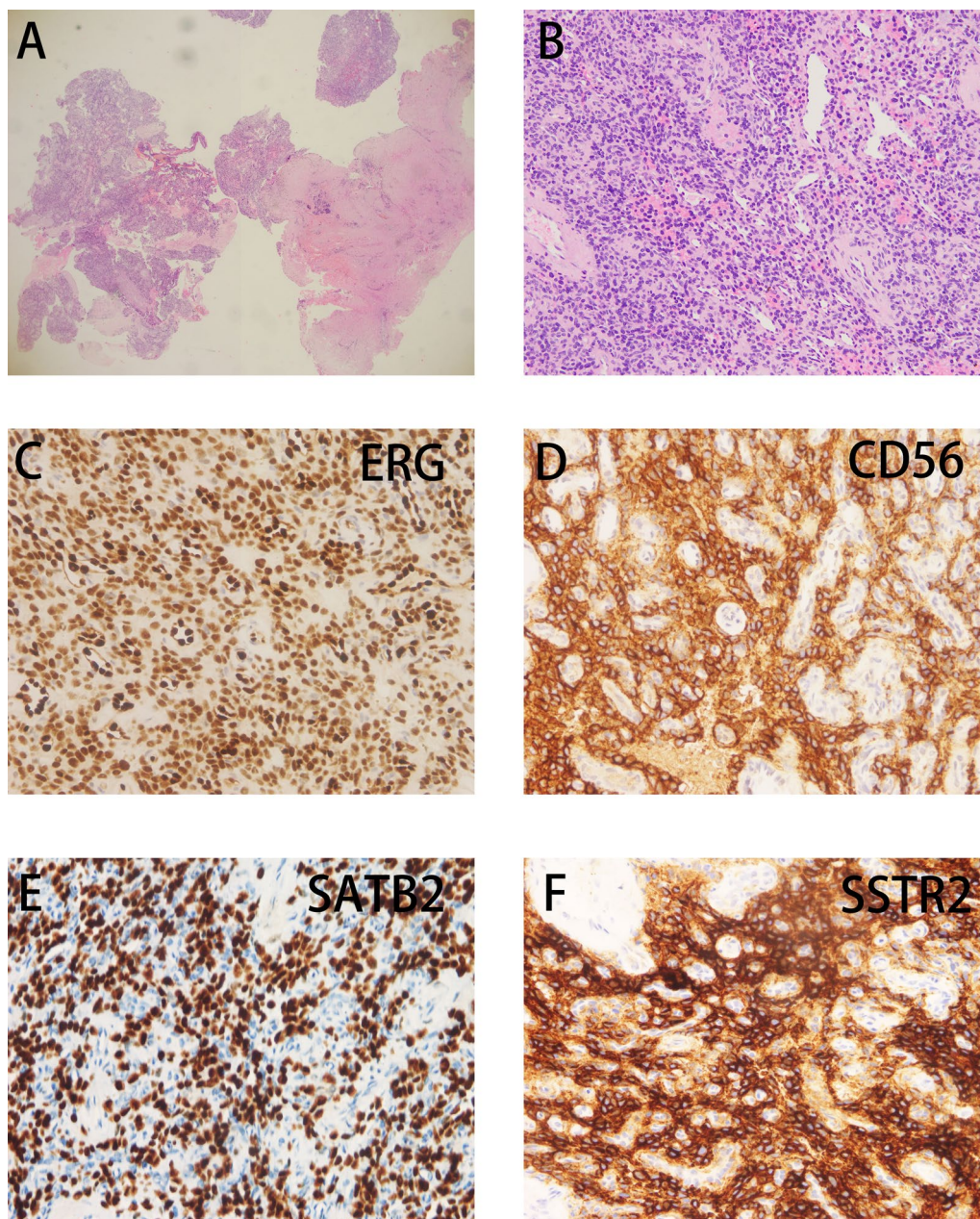


Fig. 3 Tumor tissue observed under the microscope arranged in solid sheets, with stroma rich in thin-walled or thick-walled vessels, and focal mucinous metaplasia. The tumor cells are spindle-shaped or ovoid, with approximately two mitotic figures per ten high-power fields (HPF). Immunohistochemically, the tumor shows an immunophenotype of SSTR2 (+++), ERG (+), CD56 (++), SATB2 (+++)

to be taken orally once daily, with one course lasting 14 days.

At 6 months postoperatively, the patient's serum calcium level was 2.64 mmol/L (normal range: 2.11–2.52 mmol/L), phosphate level was 0.72 mmol/L (normal range: 0.85–1.51 mmol/L), and alkaline phosphatase (ALP, not ALT) level was 127 U/L (normal range: 35–100 U/L). Follow-up MRI showed no significant signs of local

recurrence compared to the scan before surgery (Fig. 4). At the 12-month follow-up, the patient experienced significant relief from bone pain, with serum calcium and phosphate levels returning to the normal range, and no limitations in daily walking ability. At the 16-month follow-up, the patient had returned to normal work and life activities. A whole-body PET-CT scan showed no signs of tumor recurrence in the surgical area, and

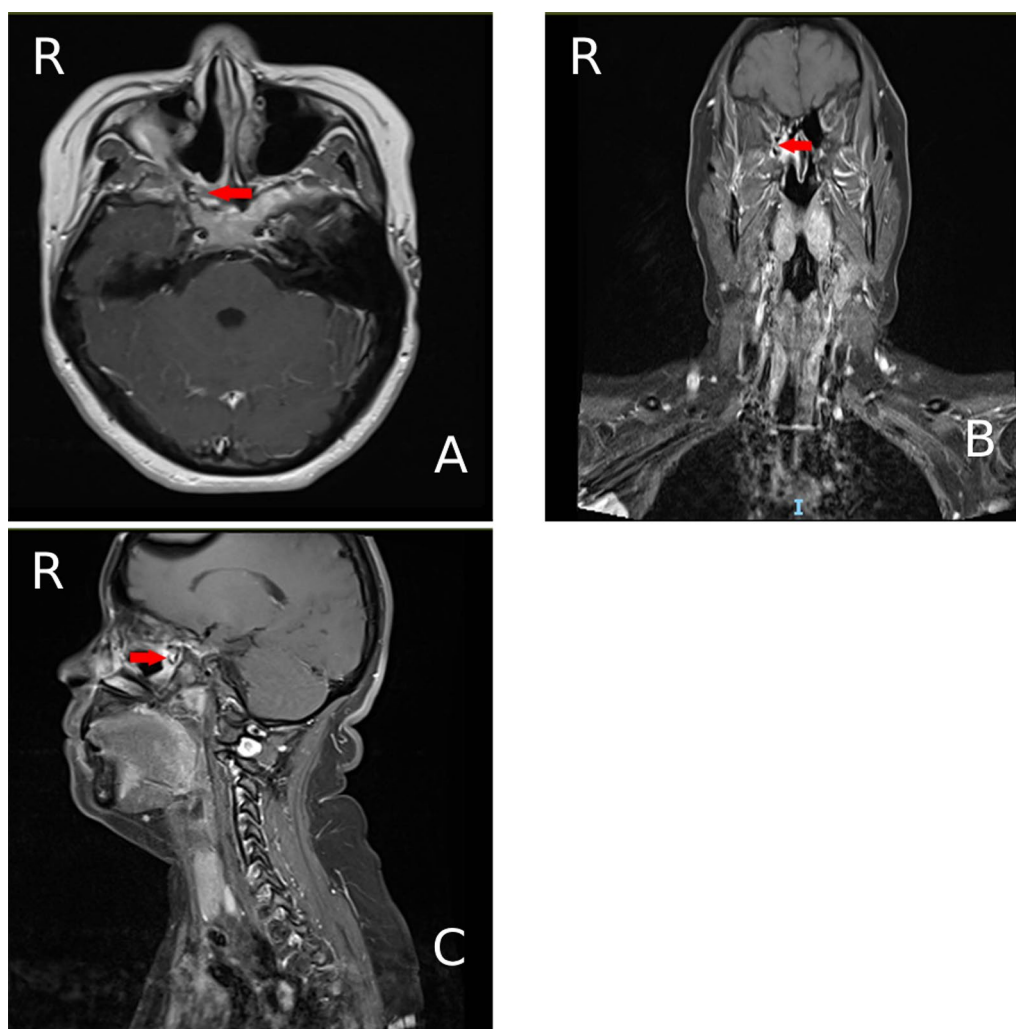


Fig. 4 Re-examination of the magnetic resonance enhancement scan, compared with the image from 21 July 2022, showing postoperative changes at the skull base lesion site following resection, with no clear signs of local recurrence observed (Arrows refer to the site where the original tumor was located)

fludeoxyglucose F18 (18 F-FDG)-PET/CT whole-body imaging did not show any malignant metabolic images in other parts of the body (Table 1).

Discussion

Patients with PMT typically present with bone pain, muscle weakness, and multiple fractures. PMTs often harbor FN1-FGFR1 (42%) or FN1-FGF1 (6%) fusions, leading to activation of the tyrosine kinase FGFR1 signaling pathway, which drives tumorigenesis and up-regulation of FGF23 expression [8]. Because tumor cells produce serum fibroblast growth factor-23 (FGF-23), renal tubular phosphate reabsorption is abnormal or reduced. The main biochemical marker findings were hypophosphatemia, normal or low serum 1, 25-dihydroxyvitamin D levels, elevated serum alkaline

phosphatase levels, and elevated or abnormal FGF-23 levels [6]. Neuroendocrine tumor cells express high levels of somatostatin receptors on their surface, which can bind specifically to somatostatin, aiding in the localization of the tumor; imaging techniques such as somatostatin receptor scintigraphy and 68 Ga-DOTA-TATE PET/CT help in localizing the tumor [9, 10].

Immunohistochemistry has limited value, and the basic diagnosis includes the combination of clinical manifestations. Most studies suggest that the immunophenotype of these tumors is typically positive for vimentin, with focal expression of CD34, SMA, PGP9.5, S100, Syn, and dentin matrix protein-1 (DMP-1) observed in some cases [1]. Recent studies also report frequent expression of SATB2, CD56, ERG, and somatostatin receptor 2A [3], with SATB2

Table 1 Laboratory data

Variable	Reference range, this hospital*	On admission	6 months after	9 months after	1 year after	1 year after	1.5 years after	2 years after
Plasma fibrinogen (g/L)	1.9–4.00	3.69	3.44	4.12	–	–	5.68	3.99
Calcium (mmol/L)	2.11–2.52	2.73	2.64	2.75	2.67	2.04	2.68	2.33
Phosphorus (mmol/L)	0.85–1.51	< 0.32	0.72	0.98	1	–	0.88	0.71
Alkaline phosphatase (U/L)	35–100	381	127	99	–	–	85	62
Uric acid (μmol/L)	208–428	458.4	468	669	653.3	–	456	547.4
White-cell count (× 10 ⁹ /L)	3.5–9.5	7.45	7.78	8.29	7.93	8.08	9.27	7.47
Hemoglobin (g/L)	115–150	131	135	170	167	155	173	144
Platelet count (× 10 ⁹ /L)	125–350	307	352	305	309	280	278	282

expression suggesting osteoblastic differentiation of the tumor. Overall, by immunohistochemistry, most PMTs expressed CD56, ERG, FGFR1, SATB2, and/or SSTR2 A.

To limit local destruction and eliminate the source of protein secretion associated with TIO, extensive complete resection with negative surgical margins is required [5]. There are currently no established standard medical treatment protocols for this tumor, and treatment strategies are typically individualized on the basis of the patient's specific circumstances and symptoms. Treatment options may include neoadjuvant chemotherapy such as doxorubicin, docetaxel, and gemcitabine [8]. In this case, anlotinib was given according to the pathological manifestations of tumor cells with hemangiopericytoid growth pattern and the patient's characteristics of multiple bone destruction. As noted in previous studies, FGFR1 expression is commonly observed in PMTs, regardless of gene fusions. Anlotinib shows potential efficacy in treating PMTs by inhibiting FGFR1 expression. During the trial period, the most common grade 3 or 4 adverse events with anlotinib were hypertension (10.0% versus 0% with placebo), elevated thyroglobulin (5.0% versus 1.8%), and hand-foot skin reaction (3.3% versus 0%). All adverse events were effectively managed by dose adjustment or symptomatic treatment, and no

treatment-related deaths occurred[11]. We will continue to have annual follow-up with the patient so that the drug dose can be adjusted at any time as side effects develop. Further study of the factors associated with effective standardized medication after surgery is needed.

A total of 23 cases of PMT in the nasal cavity, paranasal sinuses, and skull base have been reported in the literature (Table 2). Most patients (95.65%) presented with TIO manifestations, and other fractures were observed with longer disease duration. Clinical manifestations alone often lead to misdiagnosis. Following surgical treatment, most patients showed favorable outcomes, though recurrence occurred in 13.04% of cases, with some patients dying after recurrence. The case reported here is the third documented case of PMT in the skull base and the first treated with postoperative combination anlotinib [12–21].

Conclusions

Diagnosis and treatment of PMTs remains a challenge. We discuss here imaging and serologic tests that can aid in rapid diagnosis. At the same time, anlotinib capsules were used after surgery. Our case discussion provides an updated review of the evidence for optimal management of patients with PMTs, with a particular focus on novel pharmacological options that exploit underlying pathogenesis.

Table 2 Review of research on the frequency, location and therapy of PMTs

No	Age (years)/gender	Location	Phosphuria/hypophosphatemia	TIO	Treatment	Prognosis	Author, year
1	NA/F	Maxillary sinus	Yes	Yes	Surgery	Recurrence after 10 years	Allevi F, 2014
2	41/M	Nasal cavity	NA	NA	Surgery	NED 2 years	Deep NL, 2014
3	35/F	Ethmoid sinus	NA	Yes	Surgery	NED 3 years	Okamiya T, 2015
4	48/F	Nasal cavity, ethmoid, maxillary sinuses	Yes	No	Surgery	NED 1 year	Mok Y, 2016
5	53/F	Skull base	Yes	Yes	Surgery, vitamin D supplementation	NA	Basu S, 2016
6	62/F	Nasal cavity, ethmoid, frontal sinuses	NA	Yes	Surgery, EBRT	NED 1 year	Kane SV, 2018
7	56/M	Nasal cavity, ethmoid, sphenoid sinuses	NA	Yes	NA	NA	
8	52/M	Nasal cavity	NA	Yes	Surgery	NED 1 year	
9	39/M	Ethmoid, frontal sinuses	NA	Yes	Surgery	Residual disease 2 months, re-excision NED 10 months	
10	34/M	Nasal cavity, maxillary sinuses, intracalvarium	No	No	Surgery, IMRT	NED 6 months	
11	35/F	Ethmoid, frontal sinuses	NA	Yes	Surgery	NA	
12	41/F	Nasal cavity, ethmoid sinus, frontal sinus, skull base	Yes	Yes	Surgery	NED 9 months	Villepelet A, 2018
13	59/M	Nasal cavity, ethmoid sinus	Yes	Yes	Surgery	NED 12.5 months	Tang R, 2020
14	42/F	Nasal cavity, ethmoid sinus	Yes	Yes	Surgery	NED 11 months	
15	56/F	Frontal bone	Yes	Yes	Surgery	NED 10.5 months	
16	42/M	Nasal cavity, ethmoid sinus	Yes	Yes	Surgery	NED 9.5 months	
17	43/F	Ethmoid, frontal sinuses	Yes	Yes	Surgery	NED 14.5 months	
18	54/F	Nasal cavity, ethmoid sinus	Yes	Yes	Surgery	NED 2 years	
19	42/M	Nasal cavity, ethmoid sinus, intracalvarium	Yes	Yes	Surgery	Developed recurrence and died	
20	36/F	Nasal cavity, ethmoid sinus	Yes	Yes	Surgery	NED 4.5 years	
21	51/M	Nasal cavity, ethmoid sinus	Yes	Yes	Surgery	NED 5 years	
22	48/F	Sphenoid sinus, ethmoid sinus	Yes	Yes	Surgery	NED 6 months	Jawan F, 2023
23	50/F	Ethmoid sinus	Yes	Yes	Surgery	NED 10 months	Bhatia SS, 2024
24	27/F	Skull base	Yes	Yes	Surgery, anlotinib	NED 2 years	This case

Acknowledgements

Not applicable.

Author contributions

HZ and WK co-authored the manuscript, with QQ responsible for table creation and image data screening. Pathological data were provided and vetted by ZM and QJ. All authors critically revised the manuscript for intellectual content and clarity. HZ prepared the final draft, which was supervised by QQ and WK, both of whom also performed the surgery. All authors reviewed and endorsed the final manuscript.

Funding

The authors received no specific funding for this work.

Availability of data and materials

Not applicable.

Declarations**Ethics approval and consent to participate**

Approval for this study was obtained from the Department of Medicine at Southern Medical University.

Consent for publication

Written informed consent for publication of this case report and any accompanying images was obtained from the patient. The written consent is available for review by the Editor-in-Chief of this journal upon request.

Competing interests

The authors declare that they have no competing interests.

Received: 26 December 2024 Accepted: 27 March 2025
Published online: 05 May 2025

References

- Folpe AL. Phosphaturic mesenchymal tumors: a review and update. *Semin Diagn Pathol.* 2019;36(4):260–8. <https://doi.org/10.1053/j.semdp.2019.07.002>.
- Feng J, Jiang Y, Wang O, et al. The diagnostic dilemma of tumor induced osteomalacia: a retrospective analysis of 144 cases. *Endocr J.* 2017;64(7):675–83. <https://doi.org/10.1507/endocrj.EJ16-0587>.
- Agaimy A, Michal M, Chiosea S, et al. Phosphaturic mesenchymal tumors: clinicopathologic, immunohistochemical and molecular analysis of 22 cases expanding their morphologic and immunophenotypic spectrum. *Am J Surg Pathol.* 2017;41(10):1371–80. <https://doi.org/10.1097/PAS.0000000000000890>.
- Wu H, Bui MM, Zhou L, Li D, Zhang H, Zhong D. Phosphaturic mesenchymal tumor with an admixture of epithelial and mesenchymal elements in the jaws: clinicopathological and immunohistochemical analysis of 22 cases with literature review. *Mod Pathol.* 2019;32(2):189–204. <https://doi.org/10.1038/s41379-018-0100-0>.
- Deep NL, Cain RB, McCullough AE, Hoxworth JM, Lal D. Sinonasal phosphaturic mesenchymal tumor: case report and systematic review. *Allergy Rhinol (Providence).* 2014;5(3):162–7. <https://doi.org/10.2500/ar.2014.5.0100>.
- Minisola S, Fukumoto S, Xia W, et al. Tumor-induced osteomalacia: a comprehensive review. *Endocr Rev.* 2023;44(2):323–53. <https://doi.org/10.1210/endrev/bnac026>.
- Yavropoulou MP, Poulios C, Foroulis C, et al. Distant lung metastases caused by a histologically benign phosphaturic mesenchymal tumor. *Endocrinol Diabetes Metab Case Rep.* 2018;2018:18–0023, EDM180023. <https://doi.org/10.1530/EDM-18-0023>.
- WHO Classification of Tumours Editorial Board. WHO classification of tumours of soft tissue and bone, 5th ed. IARC Press, 2020.
- Kato A, Nakamoto Y, Ishimori T, et al. Diagnostic performance of 68Ga-DOTATOC PET/CT in tumor-induced osteomalacia. *Ann Nucl Med.* 2021;35(3):397–405. <https://doi.org/10.1007/s12149-021-01575-x>.
- Minisola S, Peacock M, Fukumoto S, et al. Tumour-induced osteomalacia. *Nat Rev Dis Primers.* 2017;3:17044. <https://doi.org/10.1038/nrdp.2017.44>.
- Syed YY. Anlotinib: first global approval. *Drugs.* 2018;78(10):1057–62. <https://doi.org/10.1007/s40265-018-0939-x>.
- Allevi F et al. Mesenchymal phosphaturic tumour: early detection of recurrence. *BMJ case reports vol. 2014 bcr2013202827.* 2014, <https://doi.org/10.1136/bcr-2013-202827>.
- Deep NL, et al. Sinonasal phosphaturic mesenchymal tumor: case report and systematic review. *Allergy Rhinol (Providence, R.I.)* 2014;5(3):162–7. <https://doi.org/10.2500/ar.2014.5.0100>.
- Okamiya T, et al. Oncogenic osteomalacia caused by an occult paranasal sinus tumor. *Auris Nasus Larynx.* 2015;42(2):167–9. <https://doi.org/10.1016/j.anl.2014.10.001>.
- Mok Y, et al. From epistaxis to bone pain-report of two cases illustrating the clinicopathological spectrum of phosphaturic mesenchymal tumour with fibroblast growth factor receptor 1 immunohistochemical and cytogenetic analyses. *Histopathology.* 2016;68(6):925–30. <https://doi.org/10.1111/his.12872>.
- Basu S, Fargose P. 177Lu-DOTATATE PRRT in recurrent skull-base phosphaturic mesenchymal tumor causing osteomalacia: a potential application of PRRT beyond neuroendocrine tumors. *J Nucl Med Technol.* 2016;44(4):248–50. <https://doi.org/10.2967/jnmt.116.177873>.
- Kane SV, et al. Phosphaturic mesenchymal tumor of the nasal cavity and paranasal sinuses: a clinical curiosity presenting a diagnostic challenge. *Auris Nasus Larynx.* 2018;45(2):377–83. <https://doi.org/10.1016/j.anl.2017.05.006>.
- Villepelet A, et al. Ethmoid tumor and oncogenic osteomalacia: case report and review of the literature. *Eur Ann Otorhinolaryngol Head Neck Dis.* 2018;135(5):365–9. <https://doi.org/10.1016/j.anorl.2018.07.001>.
- Tang R, et al. Surgical treatment and outcomes for sinonasal and skull base phosphaturic mesenchymal tumors. *Otolaryngol Head Neck Surg.* 2020;162(5):674–82. <https://doi.org/10.1177/0194599820904055>.
- Jawan F, et al. Tumour induced osteopenia due to phosphaturic mesenchymal sinonasal tumour presenting with delayed onset insufficiency fractures. *J Radiol Case Reports.* 2023;17(7):8–16. <https://doi.org/10.3941/jrcr.v17i7.4912>.
- Bhatia SS, et al. FGF23-secreting sinonasal tumour presenting with acute subdural haemorrhage and tumour-induced osteomalacia. *BMJ Case Reports.* 2024;17(8):e259439. <https://doi.org/10.1136/bcr-2023-259439>.

Publisher's Note

Springer Nature remains neutral with regard to jurisdictional claims in published maps and institutional affiliations.